Chain-Length-Dependent Termination Rate Processes in Free-Radical Polymerizations. 2. Modeling Methodology and Application to Methyl Methacrylate Emulsion Polymerizations

Gregory T. Russell

Institut für Physikalische Chemie der Universität, Tammannstrasse 6, D-3400 Göttingen, Federal Republic of Germany

Robert G. Gilbert* and Donald H. Napper

School of Chemistry, University of Sydney, Sydney NSW 2006, Australia

Received January 26, 1993; Revised Manuscript Received April 5, 1993

ABSTRACT: Results are presented from modeling of extensive methyl methacrylate seeded emulsion polymerization data. Both chemically initiated and γ radiolysis initiated experiments were modeled; in the latter type of experiments the system is removed from the γ-source, thereby providing kinetic data which are particularly sensitive to termination processes. While the data cannot be fitted consistently and meaningfully with conventional termination models, all are fitted in a unified way using the description of Russell *et al.* (*Macromolecules* **1992**, *25*, 2459). Fitting completely without adjustable parameters gives quite acceptable agreement with these sensitive experimental data, and exact accord is obtained with minor, and physically reasonable, parameter changes. The model description is applicable to free-radical polymerizations at intermediate and high conversion (*i.e.*, above c^{**}). Its main feature is that it takes full account of the dependence of termination rate coefficients on radical chain length, while still requiring only modest computational resources. The most important model parameters are therefore experimental diffusion coefficients for monomer as a function of weight fraction polymer, and exponents for the scaling of oligomeric and polymeric diffusion coefficients with degree of polymerization. For emulsion systems, desorption (exit) kinetics are included, and the theory of Maxwell *et al.* (*Macromolecules* **1991**, *24*, 1629) for the rate of chemical initiation is found to be accurate. The modeling indicates that the predominant mode of termination above c^{**} and prior to the glass transition involves a short free radical, usually one formed by transfer, and a long entangled macroradical; above the glass transition, this dominant model involves two long entangled macroradicals encountering as a result of propagation ("reaction diffusion"). The origin of the Trommsdorff effect is the slowing with conversion of the termination rates of shorter chains, this being brought about by the increase with conversion of viscosity and of tendency to become entangled.

Introduction

In free-radical polymerizations, termination is diffusion-controlled.[1] It is usual to distinguish between various diffusive processes which can lead to termination: (1) segmental, (2) center-of-mass, and (3) "residual", in which diffusion is through propagational growth (this process is also known as "reaction diffusion"[2]). Because the rates of each of these processes can vary with both degree of polymerization and polymer concentration, ascertaining the mechanism of termination in free-radical polymerizations is no trivial task. It is, however, important, because a qualitative and quantitative understanding of termination is of both scientific and practical importance. To take two examples, center-of-mass diffusion in polymeric (particularly glassy) media is a frontier area in chemical physics, while, on the applied side, control of termination can lead to control of molecular weight distributions, residual monomer content, and so on. The object of the present paper is to attack the problem of understanding termination in real systems at its most complex point: when termination rates are determined by the speed of center-of-mass diffusion processes, and thus termination rate coefficients are expected to depend markedly on the length of each growing chain.[1,3-11] The aim is to further understanding of this process through modeling of data which are sensitive to this effect.

Using quantitative models for polymerization kinetics can at worst be an exercise in curve fitting but, if done properly, can give both quantitative and qualitative insight into mechanisms and hence afford control and rational design of polymerization processes and properties. The major criterion which enables the latter outcome to be achieved is that the data be sufficient in scope and type to be sensitive to the mechanisms under scrutiny. The goal of the present modeling studies is to gain appropriate insight into the mechanism of termination at intermediate and high weight fraction of polymer. In this paper we therefore first emphasize data for fitting which are most sensitive to termination, *i.e.*, kinetic data that are dominated by chain-stopping, rather than chain-starting, events. Kinetic data from relaxations (otherwise known as post- or aftereffects), obtained from experiments in which the free-radical-generating flux is switched off and the decrease in polymerization rate then followed accurately, are particularly suitable for this purpose. Such modeling is rendered even more discerning if it is then applied to data obtained at the same conditions but with the radical-generating flux still operating (*e.g.*, chemically initiated polymerizations).

Data that fulfil the above criteria can be obtained using seeded emulsion polymerizations (which take place at weight fractions of polymer typically in the range from 30 to 100%). These can be initiated by a conventional persulfate system and also with γ radiolysis.[12,13] The latter permits the reactor to be removed essentially instantaneously from the radiation source. Because this leads to very rapid cessation of radical activity in the aqueous phase, the resulting relaxation kinetics (which can be followed dilatometrically, for example) will be dominated by radical-loss processes. In the usual event this is termination within the particles, although it can be exit (desorption).

We confine our attention in this paper to systems at intermediate and high polymer weight fraction, because

* Author to whom correspondence should be addressed.

0024-9297/93/2226-3538$04.00/0 © 1993 American Chemical Society

the chemical physics of diffusion-controlled termination in these systems is in some ways simpler than at high dilution. The diffusive processes in systems at low conversion are still under active investigation, without agreement as to whether kinetically important roles are played by processes such as solvent shielding and center-of-mass diffusion between chains, as distinct from the configurational rearrangements of already proximate chains (segmental diffusion). On the other hand, at intermediate conversion, the nature of diffusive processes is qualitatively different. This is because such systems have polymer concentrations well above the concentration for onset of polymer entanglement c^{**} (to use the notation of Tulig and Tirrell[5]). Thus, there are no nonoverlapping chains (as distinct from the situation at zero conversion) and all but the shortest chains are entangled, and the monomer/polymer solution effectively behaves as a Θ-system. Therefore, the dominant diffusive motion of the radical chain ends will be either center-of-mass diffusion of the whole chain or reaction diffusion if the chain is very long and its reptational motion thus slow. Despite this relative conceptual simplicity, there are insufficient data for the variation of center-of-mass diffusion coefficients with polymer fraction and with degree of polymerization to enable these dependences to be assigned unambiguously. Therefore, we are forced to be content with assuming diffusion coefficients that are as physically reasonable as possible. These will be seen to reproduce the kinetic data. However, our parameter values should not be regarded as being the absolute truth; we stress at the outset that our fitting is likely to require revision as more exact data on diffusion become available and so can be used in modeling kinetic data. We emphasize the methodology of this paper as being the detailed mechanistic way to model and so understand the complexities of the kinetics of free-radical polymerizations.

In this paper, we first summarize the model (presented in detail elsewhere[11]) of polymerization kinetics that has been used, as well as give some extensions to it and details of the numerical methods employed. The model requires a knowledge of the rate coefficients for propagation, for transfer, for the various events involved in initiation (and, for emulsion polymerization, for exit), and, for the termination processes, the diffusion coefficients of radical species as functions of weight fraction polymer (w_p) and of degree of polymerization. We then apply the model to the seeded emulsion polymerization of methyl methacrylate (MMA), starting out with data at high conversion (*i.e.*, at and beyond the glass transition), which are interpreted relatively simply, and then progressing to lower conversions, where fitting is more complex. Parameter fitting is carried out on relaxation data at a particular w_p, and the resulting parameters are tested by seeing how well the model predicts relaxation data at another w_p and chemically initiated results over a range of w_p.

Mathematical Description and Its Implementation

The most important phenomenon to account for in modeling termination processes at intermediate conversions is that the rate coefficient for terminations, k_t, depends on the degrees of polymerization i and j of the two chains involved and thus must be written k_t^{ij}. Although many formulations, of varying degrees of complexity, of the corresponding kinetic equations have been given,[3-11] we adopt here that of paper 1 in this series.[11] This formulation is detailed, uses physically reasonable models for the various processes involved, is equally adapted for bulk and emulsion systems, and requires only modest computational resources for most systems of interest. It is therefore particularly well suited for proper data fitting and prediction.

In this section, we give a minimal summary of the model so as to enable understanding of the applications of it presented in this current study. Because of the straightforward but nontrivial differences in the equations for emulsion and for bulk systems, we once again give both versions of the equations, and as before label them *a* and *b*, respectively. For our emulsion system equations we use the "pseudo-bulk" approximation,[14] which says that the effects of free radicals being compartmentalized may be ignored; this is always valid for MMA and other emulsion systems[15] in which $\bar{n}$ (the average number of free radicals per latex particle) is usually large. Our model is expressed in terms of the time evolution of the population of free radicals of degree of polymerization i, T_i. The normalization of these populations is defined to be

$$\sum_{i=1}^{\infty} T_i = \bar{n} \tag{1a}$$

$$\sum_{i=1}^{\infty} T_i = [R^\bullet] \tag{1b}$$

where $[R^\bullet]$ is the total radical concentration in a homogeneous system. The kinetic events that must be taken into account are propagation, transfer, initiation (entry in the case of emulsion polymerization), chain-length-dependent termination, and, for emulsion polymerizations, exit (desorption) of free radicals from latex particles, including accounting for the various possible fates of desorbed free radicals (aqueous-phase termination, reentry, and, once within a particle again, propagation, termination, or re-escape[16-21]). The resulting evolution equations are

$$\frac{dT_1}{dt} = \rho + k_{tr}[M]\sum_{i=2}^{\infty} T_i - k_p^{1}[M]T_1 - \beta k_{tr}[M]\sum_{i=2}^{\infty} T_i - 2T_1\sum_{i=1}^{\infty} c^{1i}T_i \tag{2a}$$

$$\frac{dT_1}{dt} = 2k_d f[I] + k_{tr}[M]\sum_{i=2}^{\infty} T_i - k_p^{1}[M]T_1 - 2T_1\sum_{i=1}^{\infty} k_t^{1i}T_i \tag{2b}$$

$$\frac{dT_2}{dt} = -k_{tr}[M]T_2 + k_p^{1}[M]T_1 - k_p[M]T_2 - 2T_2\sum_{i=1}^{\infty} c^{2i}T_i \tag{3a}$$

$$\frac{dT_2}{dt} = -k_{tr}[M]T_2 + k_p^{1}[M]T_1 - k_p[M]T_2 - 2T_2\sum_{i=1}^{\infty} k_t^{2i}T_i \tag{3b}$$

$$\frac{dT_i}{dt} = -k_{tr}[M]T_i + k_p[M](T_{i-1} - T_i) - 2T_i\sum_{j=1}^{\infty} c^{ji}T_j \qquad i > 2 \tag{4a}$$

$$\frac{dT_i}{dt} = -k_{tr}[M]T_i + k_p[M](T_{i-1} - T_i) - 2T_i\sum_{j=1}^{\infty} k_t^{ji}T_j \qquad i > 2 \tag{4b}$$

Here [M] is the monomer concentration in the locus of polymerization, k_{tr} is the rate coefficient for transfer to monomer (other types of transfer are here ignored), k_p is the rate coefficient for propagation, which may in general be dependent upon chain length, a possibility here specifically accounted for through inclusion of a monomeric free-radical propagation rate coefficient k_p^1, ρ is the overall rate coefficient (including any background thermal component[22,23]) for entry of free radicals into latex particles, $c^{ij} = k_t^{ij}/(N_A V_S)$, where N_A is the Avogadro constant and V_S the swollen volume of a latex particle, [I] is the initiator concentration, k_d is the initiator decomposition rate coefficient, and f is the initiator efficiency (for the case of bulk/solution systems).

About the above equations we here note the following: (i) We have followed the American convention for writing down rates of free-radical loss by termination. (ii) For conceptual clarity our equations for homogeneous systems ignore volume contraction upon polymerization; how this can be accounted for is both simple and well-known. We note that in this respect our emulsion system equations are exact, because they are balances in radical *number* (as opposed to radical concentration). (iii) We account for the emulsion polymerization process of exit in a way which improves on our original formulation.[11] We now allow for exit of a transferred free radical occurring through diffusion away from the particle, provided it does not propagate[16,17,20] or terminate first; the probability of successful escape is thus given by

$$\beta = \frac{k_{dM}}{k_{dM} + k_p^1[M] + 2\sum_{i=1}^{\infty} c^{1i} T_i} \tag{5}$$

where k_{dM} is the rate coefficient for diffusive escape, being given by[19]

$$k_{dM} = \frac{3D_{aq}}{r_S^2}\frac{[M_{aq}]}{[M]} \tag{6}$$

Here D_{aq} is the diffusion coefficient of a monomeric free radical in the aqueous phase, $[M_{aq}]$ the aqueous-phase concentration of monomer, and r_S the swollen radius of the latex particle. One might be tempted to use eq 6 in eq 2a instead of the given formulation for exit. To do so would, however, be inaccurate due to the physical reality that not all T_1 species (specifically, entering species) are able to undergo desorption—implicit in eq 2a is that entering species are unable to desorb. (iv) All free-radical concentrations have been assumed to be spatially homogeneous. It is conceivable that in emulsion polymerizations a radical gradient in the latex particles could exist, this due to fixing at the particle surface of the hydrophilic end-groups of initiator-derived entering species. Such an effect, which can only be operative when a significant concentration of an initiator such as $K_2S_2O_8$ is employed, is nonsimple to model.[24-26] Besides, such modeling[24-26] has indicated that for the sorts of (relatively) small particle systems looked at in this paper, radical concentrations within latex particles are homogeneous. (v) The rate coefficient for entry also takes into account re-entry of desorbed free radicals. (vi) *All* entering species (including re-entering species) are assumed to be monomeric in degree of polymerization. Points v and vi are expanded upon later in this section.

Equations 2–4 can be simplified through two approximations. The first is the steady-state approximation, which yields a set of nonlinear equations which can be solved iteratively to yield each T_i; these equations are the first of each relation given below. These steady-state equations have been further simplified below to yield a set of equations which, providing the relevant overall radical concentration is stipulated, eliminates the need for iterative solution. The assumption used here is the "short–long" approximation, which is that the rate at which a (short) chain terminates depends only on the length of the (short) chain and not on the length of the chain with which it is terminating. This assumption has been discussed at length in our earlier publication,[11] in which it was shown that under intermediate- and high-conversion conditions the assumption is very accurate. The basic reason for this is that under such conditions an overwhelming majority of termination events involve a relatively short, mobile chain and a longer entangled one that is essentially immobile in comparison. These exact and approximate steady-state solutions are

$$T_1 = \frac{\rho + (1-\beta)k_{tr}[M]\sum_{i=2}^{\infty} T_i}{k_p^1[M] + 2\sum_{i=1}^{\infty} c^{1i} T_i} \approx \frac{\rho + k_{tr}[M]\bar{n}(1-\beta)}{k_p^1[M] + 2c^{1L}\bar{n}} \tag{7a}$$

$$T_1 = \frac{2k_d f[I] + k_{tr}[M]\sum_{i=2}^{\infty} T_i}{k_p^1[M] + 2\sum_{i=1}^{\infty} k_t^{1j} T_i} \approx \frac{2k_d f[I] + k_{tr}[M][R^\bullet]}{k_p^1[M] + 2k_t^{1L}[R\bullet]} \tag{7b}$$

$$T_2 = \frac{k_p^1[M]T_1}{k_p[M] + k_{tr}[M] + 2\sum_{i=1}^{\infty} c^{2i} T_i} \approx \frac{k_p^1[M]T_1}{k_p[M] + k_{tr}[M] + 2c^{2L}\bar{n}} \tag{8a}$$

$$T_2 = \frac{k^{p1}[M]T_1}{k_p[M] + k_{tr}[M] + 2\sum_{i=1}^{\infty} k_t^{2i} T_i} \approx \frac{k^{p1}[M]T_1}{k_p[M] + k_{tr}[M] + 2k_t^{2L}[R^\bullet]} \tag{8b}$$

$$T_i = \frac{k_p[M]T_{i-1}}{k_p[M] + k_{tr}[M] + 2\sum_{j=1}^{\infty} c^{ji} T_j} \approx \frac{k_p[M]T_{i-1}}{k_p[M] + k_{tr}[M] + 2c^{iL}\bar{n}} \quad i > 2 \tag{9a}$$

$$T_i = \frac{k_p[M]T_{i-1}}{k_p[M] + k_{tr}[M] + 2\sum_{j=1}^{\infty} k_t^{ji} T_j} \approx \frac{k_p[M]T_{i-1}}{k_p[M] + k_{tr}[M] + 2k_t^{iL}[R^\bullet]} \quad i > 2 \tag{9b}$$

In view of the proven accuracy of the short-long approximation, a logical follow-on to it is to consider all radicals of chain length $i > Z$ as being kinetically identical. Thus, all such radicals can be considered as a single, "long" (hence the symbol L) free-radical population, whose population balance equation replaces eqs 2–4:

$$\frac{dT_L}{dt} = k_p[M]T_Z - k_{tr}[M]T_L - 2c^{LL}T_L^2 - 2T_L\sum_{i=1}^{Z} c^{iL}T_i \quad (10a)$$

$$\frac{dT_L}{dt} = k_p[M]T_Z - k_{tr}[M]T_L - 2k_t^{LL}T_L^2 - 2T_L\sum_{i=1}^{Z} k_t^{iL}T_i \quad (10b)$$

In using eqs 10a,b, the populations of species for which $i \leq Z$ are given by eqs 7–9. The parameter Z, marking as it does the boundary between short and long chains in *model* terms, can crudely be thought of, if one insists on trying to give it a physical meaning, as the degree of polymerization at which chains become entangled. However, in actuality Z is no more than a numerical parameter which must be made sufficiently large that the solutions to the above equations become independent of its value. We note that the approximation of putting T_L equal to $\bar{n}$ and [R•], respectively, enables still further simplification of eqs 10; such a move has been shown for intermediate conversion conditions to result in reasonably accurate approximations to the exact kinetics.[11]

Numerical solution of all of the above equations, either exact or approximate, can be made more efficient through (coarse) graining: this is equivalent to expressing these equations in integral terms and using finite-difference forms. Details of the general method have been given in paper 1.[11] Not given in paper 1 were the exact steady-state solutions to the coarse-grained population balance differential equations:

$$P_I = \frac{k_p[M]P_{I-1}/\Delta_I}{(k_p[M]/\Delta_I) + k_{tr}[M] + 2\sum_{J=1}^{\infty} c^{JI}P_J\Delta_J} \qquad I > 2 \quad (11a)$$

$$P_I = \frac{k_p[M]P_{I-1}/\Delta_I}{(k_p[M]/\Delta_I) + k_{tr}[M] + 2\sum_{J=1}^{\infty} k_t^{JI}P_J\Delta_J} \qquad I > 2 \quad (11b)$$

Here the coarse-grained variable P_I is

$$P_I = \sum_{i\in\Delta_I} T_i \approx T_i(\text{any } i \in \Delta_I)|\Delta_I| \quad (12)$$

i.e., P_I is the summed value of T_i over the Ith grain, which is of size $|\Delta_I|$, *etc.* The equations for the special cases of $I = 1$ and 2 have not been given above, because in practical modeling it is recommended that monomeric and dimeric free radicals always be treated as individual species (as indeed we did in this study). In this event the grain size for $I = 1$ and 2 species is one monomer unit, and thus the relevant grained relations are the same as eqs 7 and 8. On this point, we note that for the actual modeling of this work coarse-grained analogs of the exact population balance equations (eqs 2a–4a in the case at hand of emulsion polymerization) were used. The resulting set of coupled differential equations were solved numerically using the Gear algorithm (including an extra equation for conversion). However, these more detailed calculations showed that eqs 7–10 are perfectly acceptable for exact, microscopic modeling of intermediate and high conversion polymerizations, whose accuracy has been conclusively proven.[11]

To conclude this section, we stress that it is important to be aware that the strong dependence of the termination rate coefficient upon chain length implies that the usual second-order termination kinetics, *viz.*

$$\frac{d\bar{n}}{dt} = \rho - \beta k_{tr}[M]\bar{n} - 2c\bar{n}^2 \qquad \frac{d[R^\bullet]}{dt} = 2fk_d[I] - 2k_t[R^\bullet]^2 \quad (13)$$

will in general be invalid (except in the glassy regime, as shown later). However, a formal *average* termination rate coefficient can be defined

$$\langle k_t \rangle = \sum_i\sum_j k_t^{ij}T_iT_j/(\sum_i T_i)^2 \quad (14)$$

so that eq 13 is always obeyed. However, it must be recognized that this $\langle k_t \rangle$ depends not only upon w_p and all other parameters with which the k_t^{ij} vary but also on the T_i themselves and so on factors such as initiator concentration. Equation 14 further means that for *exact* and *microscopic* modeling of polymerizations, the superficially simple eq 13 is useless without knowledge of the entire living radical distribution.

Entry for Emulsion Polymerization Systems. For the case of emulsion polymerization systems, we give the requisite results for the entry of initiator-derived free radicals and for the fate of desorbed free radicals in the aqueous phase, both of which contribute to the overall entry rate coefficient. This overall entry rate coefficient ρ will be the sum of contributions from each source. For entry by free radicals arising directly from initiator, the model of Maxwell *et al.*,[27] which has been shown to reproduce a wide range of data on initiator efficiency in emulsion polymerizations,[20,27] can be used. The model assumes that entry occurs if and only if an oligomeric radical formed by aqueous-phase propagation of the product of initiator decomposition attains a critical degree of polymerization z in the aqueous phase. To a very good approximation, the final result of this model is[27]

$$\rho_{\text{initiator}} = \frac{2k_d[I]N_A}{N_c}\left\{\frac{2(k_d[I]k_{t,aq})^{1/2}}{k_{p,aq}[M_{aq}]} + 1\right\}^{1-z} \quad (15)$$

where N_c is the number concentration of latex particles, $k_{p,aq}$ and $k_{t,aq}$ are the propagation and termination rate coefficients in the aqueous phase, and $[M_{aq}]$ is the monomer concentration in the aqueous phase.

Next, the fate of free radicals which have desorbed (exited) into the aqueous phase must be taken into account. While there is a considerable body of literature on this,[13,16,18,19,23,28–30] we here adopt the results of recent theory and experiment.[17,20,21] These results, based on new data and a rationalization of literature results, show that for monomers such as styrene and MMA, at least, desorbed free radicals arise from transfer inside the latex particles[31] and that their most likely fate in the aqueous phase is to re-enter another particle and remain therein. The final result is simply therefore to add a re-entry component to ρ given by

$$\rho_{\text{re-entry}} = k_{tr}[M]\beta\sum_{i=2}^{\infty} T_i \quad (16)$$

If there is some aqueous-phase termination of desorbed free radicals, then $\rho_{\text{re-entry}}$ will be reduced below the value predicted by eq 16.

Lastly, it is necessary to add contributions to the entry rate coefficient from what has been denoted "background thermal entry".[23,32] The origin of this effect is as yet unclear (it may perhaps arise from processes on the surface of the latex particle), but it needs to be taken into account in accurate data treatment. This is most simply carried out as a component to ρ, ρ_{thermal}. The final result for entry thus is

$$\rho = \rho_{\text{initiator}} + \rho_{\text{re-entry}} + \rho_{\text{thermal}} \tag{17}$$

As eqs 2a and 17 stand, all entering species have been taken as being monomeric in degree of polymerization. One of the advantages of the chain-length-dependent approach to modeling is that this assumption need not be made: eqs 2a, 3a, and 4a can trivially be altered to allow for any variety in the lengths of the various entering species, and this was in fact done. With regard to the simplification that has here been made, there seems little doubt that the re-entry and background thermal entry processes produce monomeric free radicals. This is also expected to be the case for the entering species produced by the action of γ-radiolysis. However, from the above discussion it is clear that the entering species that result from decomposition of a chemical initiator are in fact oligomeric (perhaps tri- or tetrameric) in length, and simulations indeed revealed that model kinetics can be affected by what degrees of polymerization such entering species are assigned. However, none of the modeling results of this paper were sensitive in this respect; hence, the simplified presentation given here. This insensitivity arises because even with chemical initiator, most of the short free radicals are formed by transfer rather than entry in these systems. This aside, it is clear that in the general instance $\rho_{\text{initiator}}$, $\rho_{\text{re-entry}}$, and ρ_{thermal} should be written separately into eqs 2a, 3a, and 4a as appropriate.

Model for Termination Rate Coefficients

Because termination is diffusion-controlled, we take the Smoluchowski equation as our starting point for specifying k_t^{ij}:

$$k_t^{ij} = 2\pi p D_{ij}(r_i + r_j) \tag{18}$$

Here D_{ij} is the mutual diffusion coefficient for diffusion of the radical ends of an i-mer and a j-mer, $(r_i + r_j)$ is the radius of interaction for termination, and p is the probability of reaction upon encounter (p may be less than one because of the effects of spin multiplicity, discussed below, or any other factors which make reaction noninstantaneous once "capture" has occurred). We begin by treating the question of how to specify $(r_i + r_j)$. Consider, first, termination between two monomeric free radicals. The distance at which reaction occurs can be identified with the position of the transition state for such a radical–radical combination. Variational transition-state theory for the corresponding gas-phase reaction shows[33] that, to a reasonable approximation, $(r_i + r_j) = \sigma$, where σ is the Lennard-Jones diameter of a monomer unit, and that combination occurs with high probability whenever the two entities approach within this distance. However, termination in a polymerizing system is a condensed-phase process. The solvent cage in such circumstances is also of size σ. Thus, whenever two monomeric species approach within such a distance, they will be temporarily trapped within this cage, and so termination will occur.

Now consider termination between a monomeric free radical and a long chain. The motion of the monomeric free radical is so rapid that, on the time scale of this motion, the long chain can be thought of as immobile. Because some avenues of approach to the free-radical end of the long chain will be blocked by the long chain itself, it may be that $(r_i + r_j) < \sigma$. However, the terminal units (say the last two or three monomer units) of the long chain will certainly undergo some motion on the time scale of the approach of a monomeric free radical, and so it is speculated that this limited flexibility will compensate for the blocked avenues of approach and render $(r_i + r_j) = \sigma$ a good approximation. Next consider termination involving a longer, but still relatively short, chain—a 10-mer, for example. For such a small chain to undergo termination with another 10-mer, encounter of the free-radical ends of these two species must take place. At intermediate conversions, it is not expected that the two oligomers will remain close on the time scale of tumbling of the oligomers as a whole. In other words, because of the relatively concentrated environment of polymer, the rotation of the oligomer as a whole will not be a very rapid process relative to that of center-of-mass translational diffusion of a 10-mer over a length scale of the dimensions of a 10-mer. Hence, $(r_i + r_j)$ is not expected to be significantly greater than σ in this case. Similar arguments hold when the termination of a 10-mer with a long chain is considered: the end of the long chain will be relatively rigid on the time scale of center-of-mass diffusion of the 10-mer, the 10-mer will not be able to tumble rapidly as it passes the end of the long chain, and so $(r_i + r_j) \approx \sigma$ is reasonable. Lastly, two very long chains will terminate by reaction diffusion. We therefore expect the ends of such long chains to be relatively rigid, and so $(r_i + r_j)$ will be of the order of σ, this being the so-called rigid chain limit[34] for residual termination. In fact, in our model for residual termination interactions we allow for reasonable variation of $(r_i + r_j)$ about this value of σ. As it turns out, simulations indicate that free-radical annihilation at intermediate conversions is dominated by short–long termination, which means that it is most important to estimate $(r_i + r_j)$ accurately for short–long interactions, and for such interactions the above discussion indicates $(r_i + r_j) \approx \sigma$ to be reasonable.

Given the above discussion and the complete absence of any specific information, we have used

$$(r_i + r_j) = \sigma \tag{19}$$

for all pairs of chain lengths. Of course, our modeling method is perfectly capable of incorporating exact information, should it come to hand, on any chain-length dependences of $(r_j + r_j)$.

Now we turn to the mutual diffusion coefficient D_{ij}: it is partitioned into a sum of contributions from each of the two reacting species:

$$D_{ij} = D_i + D_j \tag{20}$$

When termination is considered, it is the rate of diffusion of the chain end, not of the center of mass of the chain, that is of interest. The relatively rapid small length scale motions of the free-radical chain end itself can be ignored in specifying D_i, for these motions will not effectively serve to bring two widely separated (on the length scale of these rapid conformational motions) free-radical chain ends any closer. Hence, only the longest length scale motion of a chain end need be considered. Two mechanisms contribute to this motion: center-of-mass diffusion of the chain as a whole, with diffusion coefficient D_i^{com}, and diffusion by propagational growth of the chain end (reaction diffusion), with diffusion coefficient D_i^{rd}. Hence

$$D_i = D_i^{com} + D_i^{rd} \tag{21}$$

The description of Russell *et al.*[34] can be used for specifying D_i^{rd}

$$D_i^{rd} = {}^1/_6 k_p[M]a^2 \tag{22}$$

where a is the root-mean-square end-to-end distance per square root of the number of monomer units in a polymer chain (*i.e.*, a is the mean distance moved, in a random flight sense, at each propagation step). The above expression is independent of the degree of polymerization, except for a dependence of k_p on i for extremely short chains, but for such i center-of-mass diffusion is so much faster than reaction diffusion that this effect can be ignored. We can thus write D^{rd} rather than D_i^{rd}.

At this juncture it should be noted that Russell *et al.*[34] also derived what was termed a "flexible chain limit" as a model for residual termination, and this limit was supposed to be applicable at lower values of w_p, when the chain ends are somewhat more exploratory in their motions than at higher w_p. However, our subsequent examination of chain-length-dependent termination[11] implies that, at lower w_p (before the glass transition), termination will be dominated by encounters between long and short chains rather than by reaction diffusion encounters between two immobile long chains. Thus, in the regime where the flexible chain expression would come to prominence, there is expected to be only minor contribution to the termination kinetics from reaction diffusion.

It remains to specify the chain-length variation of D_i^{com}. Because we are treating concentrations mostly well above c^{**}, it is reasonable to give D_i^{com} self-diffusion coefficient values. Even given this slight simplification, data in any way comprehensive are lacking on the question of the variation with degree of polymerization of the (self-)diffusion coefficient of an oligomer in a polymer matrix, although some information is beginning to emerge.[35] We here present two alternatives for specifying D_i^{com}.

(1) For long chains in concentrated polymer solutions, there is much experimental and theoretical evidence that D_i^{com} scales as the inverse square of the length of the chain:[36] this is known as the reptation[37-39] result for polymer diffusion. For the other extreme of short free radicals, matters do not seem to be so clear. In terms of the Stokes–Einstein equation, D_i^{com} might be expected to vary inversely with the *size* (as opposed to the degree of polymerization) of a small radical. At concentrations below c^{**}, this diffusional size is expected to simply reflect the overall three-dimensional size of the oligomeric species, and thus D_i^{com} would scale with the square root of chain length. However, at concentrations above c^{**}, *i.e.*, those which interest us, the high polymer concentration may force even short free radicals to diffuse along their own contour (although the short species are not entangled as such), in which event D_i^{com} will scale inversely with chain length. This result is entirely consistent with the physical picture on which reptation theory is based, the only difference being that the species being considered here are not entangled. In addition to this, there is evidence suggesting that above the dilute solution regime D_i^{com} may scale inversely with chain length for small chains. For example, Tirrell[36] mentions that experiments indicate that D_i^{com} scales as $M^{-1/2}$ to M^{-1} (M being the molecular mass of the polymer), where M is small and the concentration of polymer is low. Also, Wheeler *et al.*[40] found results that "implied the existence of a Rouse regime (*i.e.*, D_i^{com} scaling as M^{-1}) at intermediate concentrations". In summary, our model here is that for above c^{**}, $D_i^{com} \propto M^{-1}$ for small M and $\propto M^{-2}$ for large M, although the first result is far more uncertain that the second. Although the crossover with chain length from one diffusion regime to the other will be gradual in reality, for the present modeling it is assumed that the scaling exponent changes abruptly at a particular degree of polymerization X_c. Defining the diffusion coefficient of monomeric free radicals as D_{mon}, and noting that the variation of D_i^{com} with M must be continuous at both $i = 1$ (where one must have $D_i^{com} = D_{mon}$) and $i = X_c$, one has

$$D_i^{com}(w_p) = \frac{D_{mon}(w_p)}{i} \qquad i \le X_c$$
$$= \frac{D_{mon}(w_p)X_c}{i^2} \qquad X_c < i \tag{23}$$

It is stressed that the above equation is not intended for use in modeling of low conversion polymerizations. Also, in our simulations, for coarse grains of size larger than one monomer unit, i in eq 23 was taken as being the smallest $i \in \Delta_I$.

Next, we estimate X_c, the critical degree of polymerization for onset of the reptational power law for center-of-mass diffusion. Once again there do not seem to be reliable data on this at present, although hope for its determination is offered through possible measurement of D_i^{com} for monodisperse oligomeric samples, for example, by pulsed-field gradient NMR. One option is simply to treat X_c is an adjustable parameter. A slightly more sophisticated approach is to assume that the variation of this dynamic quantity with w_p is given by the same relationship as that for the similar (but not identical) topological quantity of the entanglement spacing:[41]

$$X_c = X_c^0/\phi_p \tag{24}$$

Here ϕ_p is the volume fraction of polymer, and the 100% polymer value X_c^0 is to be taken as an adjustable parameter; the relationship of the volume and weight fractions polymer is obtained by assuming volume additivity: $\phi_p^{-1} = [d_P/(d_M w_p)] + 1 - (d_P/d_M)$, where d_M and d_P are the densities of monomer and polymer, respectively. We complete this model for specificying D_i^{com} by noting that in this work the X_c given by eq 24 was not restricted to integer values.

(2) An alternative small chain dependence of D_i^{com} on i is as follows. The small chain scaling law for center-of-mass diffusion used in eq 23 obviously suffers from some inadequacies: it does not approach the limiting $i^{-1/2}$ behavior at infinite dilution (even if not intended for use here under such conditions). As an alternative, for small chains one might postulate[35]

$$\frac{D_i^{com}(w_p)}{D_{mon}(w_p)} = \frac{1}{i^\alpha} \qquad \alpha = \min\left(2, \frac{1}{2} + \frac{3}{2}\frac{w_p}{w_p^*}\right) \tag{25}$$

where w_p^* is the value of w_p at which the glass transition occurs. Equation 25, while quite empirical, has the property of yielding the above-mentioned limiting behaviors. Moreover, it is semiquantitatively in accord with new data on diffusion of oligomeric species in polystyrene.[35] Figure 1 compares the w_p dependences predicted by eqs 23 and 24, on the one hand, and eq 25, on the other, for $i = 2$ and 5 (*i.e.*, dimeric and pentameric free radicals). For use of eqs 23 and 24, $X_c^0 = 1$ (as essentially found in data fitting which is discussed later) was taken, and $w_p = \phi_p$ was assumed for the sake of simplicity. The w_p range of Figure 1 is that germane to this paper. It can be seen that the two dependences are very similar, although in this

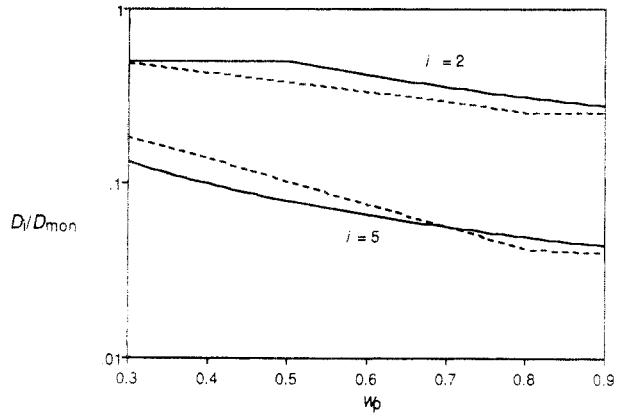

Figure 1. Comparison for $i = 2$ and 5 of $D_i(w_p)/D_{mon}$ as predicted by eqs 23 and 24 using $X_c^0 = 1$ and $\phi_p = w_p$ (full lines) and by eq 25 (broken lines).

case eq 23 may overestimate the diffusion coefficient of the dimeric species. One should bear this in mind in performing modeling, for it is the diffusion of short chains that most strongly influences intermediate conversion modeling results.

Equation 25 still leaves one with the problem of the variation of the exponent α with chain length (as opposed to with w_p): at what chain length X_c does the reptation power law set in, and how abrupt is the crossover to this dependence? In this work we adopt the semiempirical form of eq 23 for $D_i^{com}(w_p)$, recognizing that the interferences drawn from the present data fitting may require revision as more extensive data on $D_i^{com}(w_p)$ become available.

Effect of Spin Multiplicity. The following gives an important and new extension to the basic[11] theory of chain-length-dependent termination. A complication in the use of the Smoluchowski equation for radical recombination reactions is that account must be taken of spin multiplicity:[33] each radical (being a doublet) can be in one of two possible spin states. The probability is thus one in four that two free radicals will have opposite spin and so be able to combine (remembering here that combining identical spins gives three possible triplet states, whereas when opposite spins are combined, only one singlet state is possible). Hence, the encounter rate coefficient given by the Smoluchowski equation *might* need reduction by a factor of one-fourth to give the true termination rate coefficient. However, in the condensed phase, two adjacent free-radical ends may be trapped within a restraining solvent cage for a long time on the time scale of spin flipping. If any spin changes were necessary to allow reaction, these would then have sufficient time to occur before either radical end escaped the solvent cage. In this case the factor of one-fourth would not be used. Now, there is no definitive information on this question, which determines the probability factor p in eq 18, for termination by combination of polymeric radicals. Nevertheless, it seems likely that, at high conversions at least, the residence time of the radical ends within the solvent cage is sufficient for any necessary spin flips to occur. A typical spin–orbit coupling (which is what allows spin flipping to occur) for first-row elements is of the order of 10^2 cm^{-1}, which gives a very rough estimate of *ca.* 1 ps for the time between spin flips. This is of the order of what might be expected for the duration of solvent cage trapping in simple liquids. In a glassy polymeric system, much longer cage trapping is to be expected. Hence, for high conversions it seems certain that $p = 1$. The value of p before the glass transition is unknown, except in that $0.25 \leq p \leq 1$. This quantity will therefore be used as an adjustable parameter. We note that this quantity always appears as the product pD_{mon}, so that these two quantities, although physically quite distinct, can be fitted as their product where appropriate.

Parameter Values for MMA

We apply the model given above to MMA seeded emulsion polymerization data previously obtained[15,42] at 50 °C; we look at γ-radiolysis relaxations as well as systems initiated by γ-radiolysis and $K_2S_2O_8$, respectively. For γ initiation and relaxation experiments, latex particles of unswollen radii 75 nm were used, while 37- and 46-nm particles were employed for chemically initiated experiments. The γ-initiated runs involved multiple insertions and removals from the radiation source, so that the relaxations (removals) of a single run enable polymerization over a range of w_p values to be studied. In carrying out modeling, our preference is to compare simulated and experimental conversion time data, as opposed to rate time data. This is because it is actually conversion time data that are directly yielded by experiments. Additionally, rate time data are obtained by numerical differentiation of conversion time data, and thus the former must be noisier than the latter, therefore making the former less discriminatory in the modeling process. This increased noise aside, it is true that rate time data can *appear* to provide a more sensitive test of model predictions than can conversion time data, but this can be overcome simply by ensuring that conversion time data are examined closely enough. This was confirmed in a few cases in which we compared "experimental" and simulated rate time data: our conclusions from modeling conversion time data were exactly echoed by the corresponding rate time results.

It will emerge that MMA emulsion systems are sufficiently well characterized that the only parameter values in our modeling that are adjustable are the following: the value of k_p^1 (which might be an order of magnitude more than that of k_p); the product pD_{mon} of eq 18 (the value of p must lie between 1 and 0.25, while the uncertainty in D_{mon} is only slight, as discussed below); the thermal component of entry, $\rho_{thermal}$; the value of X_c; the value of σ for residual termination; the value of β, the probability that a monomeric free radical formed by transfer desorbs (counteracting this uncertainty, it is expected that, for MMA, all desorbed free radicals re-enter another particle,[20,21] in which event fitting will be insensitive to the value of β, because it has been assumed that compartmentalization effects can be ignored (this is the pseudo-bulk approximation)); re-entry (In high conversion MMA experiments $\bar{n}$ is very high and so leads to very high exit rates and thus to high aqueous-phase exited radical concentrations. Under such circumstances it is not unreasonable to allow the possibility of a small amount of aqueous-phase termination of desorbed free radicals; this means $\rho_{re\text{-}entry}$ must be slightly reduced below the value given by eq 16).

Propagation and Transfer. The data used for fitting include conditions where the system goes through the glass transition. Both propagation and transfer become diffusion-controlled under such conditions (that transfer becomes diffusion-controlled has only recently been realized[43] and arises because the transfer reaction competes with propagation). Thus one must write

$$\frac{1}{k_p} = \frac{1}{k_{diff}} + \frac{1}{k_p^0} \tag{26}$$

Here k_p^0 is the "chemically controlled" value of the

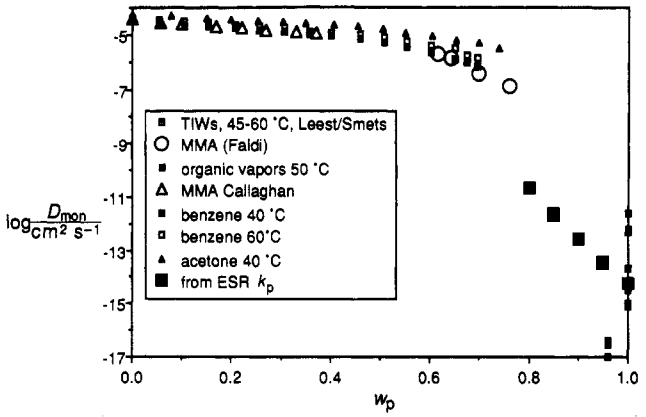

Figure 2. D_{mon} as function of w_p for MMA in poly(MMA) at 50 °C, from EPR k_p data[44,50,60] and from various literature measurements on tracer molecules.[49,51-54]

propagation rate coefficient (*i.e.*, the value at low w_p), and the diffusion-controlled component is given by

$$k_{diff} = 4\pi N_A(D_{mon} + D^{rd})\sigma \qquad (27)$$

(We note that because the values of the high-conversion monomeric diffusion coefficient D_{mon} used in eq 27 were derived[44] directly from high-conversion experimental measurements of k_p, eqs 26 and 27 are no more than a microscopic way of presenting the actual experimentally measured variation of k_p with w_p.) The transfer rate coefficient is given by[43]

$$\frac{1}{k_{tr}} = \frac{1}{k_{tr}^0}\left(\frac{k_p^0}{k_{diff}} + 1\right) \qquad (28)$$

where k_{diff} is the same as in eq 27. Equations 26 and 28 have of course the property of reducing to their chemically controlled values at low w_p, and in fact these values hold up to w_p values within a few percent conversion of the glass transition.

The value of k_p^0 for MMA at 50 °C was taken as 580 dm^3 mol^{-1} s^{-1},[45,46] and that of k_{tr}^0 was taken as 3.3×10^{-2} dm^3 mol^{-1} s^{-1}.[47]

A significant problem in the simulations is that the value of k_p^1 (the propagation rate coefficient for a monomeric free radical) is unknown for MMA (and indeed thus far for any monomer). Although it is not unreasonable on simple steric grounds alone to suppose that this quantity could well be significantly greater than the long-chain value k_p (for which there is also some indirect experimental evidence[48]), for the present simulations we have (1) first assigned k_p^1 the same value as k_p, rather than treating it as an adjustable parameter, and as an alternative (2) assigned k_p^1 a value of $10k_p$. If, as expected, k_p^1 is significantly greater than k_p (and perhaps k_p^2 could be as well), then the effect would be to increase the value of X_c and/or pD_{mon} that would be needed to fit the data.

Diffusion Coefficients and Spin-Orbit Transition Probability. For intermediate conversions, values of D_{mon} as function of w_p for MMA at 50 °C were taken from pulsed-field gradient (PFG) NMR measurements on the MMA molecule itself.[49] For high conversions at and beyond the glass transition, D_{mon} was deduced from EPR k_p data.[44,50] These data are presented in Figure 2, in which, partly for comparison purposes, diffusion coefficient data for various tracer species in poly(MMA) are also presented.[51-54] It is apparent from all of these data that the glass transition for an MMA/poly(MMA) system at 50 °C occurs at a value of w_p of about 0.82. For computational modeling purposes, the intermediate conversion D_{mon} data were represented by a fit of a standard free volume diffusion expression to the experimental data,[50] while the high-conversion D_{mon} values were expressed through a fit to the experimental $k_p(w_p)$ values.[50] One would not expect that the diffusion coefficient of a monomeric free radical would deviate greatly from that of the expressions used.

The value of σ was taken as 0.59 nm and that for a as 0.69 nm.[34]

The value of X_c was adjusted to fit the data. It will emerge that the data are only sensitive to the value of this quantity at intermediate conversions (before the system becomes glassy). It was found that with seemingly reasonable values for all other parameters, intermediate conversion data required $X_c = 1$ to be reproduced. This is admittedly a surprisingly low value; however, in appraising this result we should emphasize that X_c is not an entanglement length as such but rather the degree of polymerization above which the reptation power law for diffusion is obeyed. Unfortunately, our modeling result cannot be checked against any experimental data. However, Figure 1 suggests that $D_i^{com}(w_p)$ for this value of X_c, is, for very short species, semiquantitatively in accord with the dependence given by eq 25, which in turn is in accord with very recent data for styrene,[35] admittedly a different monomer to that studied here.

As already discussed, the value of the reaction probability p must be 1 for a glassy system but could be as low as 0.25 at lower conversions (assuming p is only influenced by spin coupling considerations).

Entry Rate Coefficient. The kinetics of entry depend on the initiator. For γ relaxation, there is only the thermal component $\rho_{thermal}$ in eq 17. This is very small for MMA latexes of the type under investigation,[15] and often (when $\bar{n}$ is large) kinetic behavior in these systems is insensitive to its value; where appropriate, it is here taken as an adjustable parameter. Although the model expressed in eq 15 could have been employed to estimate $\rho_{initiator}$ for chemically initiated experiments, instead it was decided here to fit values of $\rho_{initiator}$ and use these to test the accuracy of eq 15.

Kinetics of Exit and Re-Entry. For MMA, the rate of desorption k_{dM} is quite rapid because of the relatively high solubility of the monomer in the aqueous phase.[15] In fact, estimates of the value of the probability of exit, β, for MMA show that it is extremely close to unity for latex particles of the sizes under consideration,[15] although admittedly these calculations neglected the termination term in eq 5. For the purposes of clarity it therefore seems reasonable to put $\beta = 1$ in our modeling, particularly when one remembers that in the pseudo-bulk systems that are treated here the value of β is kinetically irrelevant in the (likely) event of there being complete re-entry. On this point there is evidence that in standard MMA systems, no matter what the initiation conditions, desorbed free radicals are far more likely to re-enter another particle than they are to undergo aqueous-phase termination;[15] this is the result of eq 16. Thus, in the general instance eq 16 is to be used. However, in some of the high conversion systems studied here, $\bar{n}$ is very high. Coupled with a value of $\beta = 1$, this gives a very high flux of desorbed free radicals, which makes it not unreasonable to postulate a little aqueous-phase termination of desorbed radicals.

Monomer Concentrations. Most data examined here were obtained in "interval III",[55] *i.e.*, in the absence of a separate monomer droplet phase. MMA has a moderate solubility in the aqueous phase, and in modeling it is important that account be taken of that fact that not all MMA resides in the particles. This can be done through

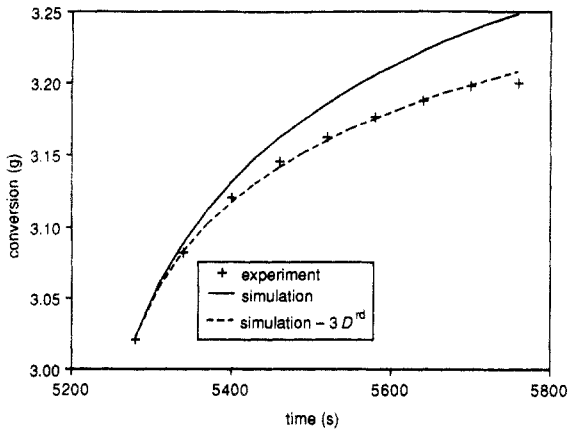

Figure 3. (Points) Conversion as function of time for relaxation experiment that was the fifth removal from source of run RG13 of Ballard *et al.*[15,42] Initial w_p was 0.88, initial $\bar{n} \approx 61$. (Lines) Simulations; (full line) parameters as in text; (broken line) as for full line but with D^{rd} increased by a factor of 3 above that predicted by eq 22.

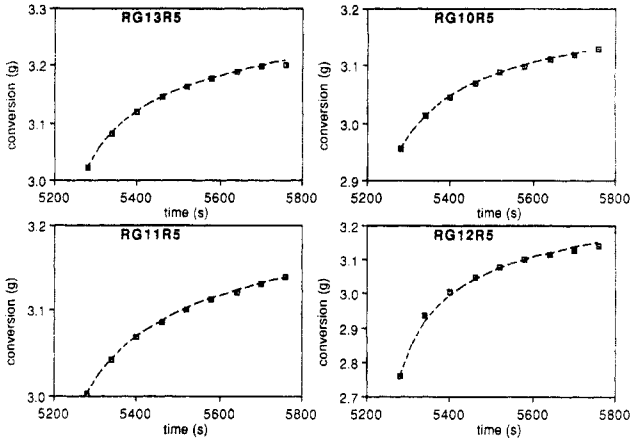

Figure 4. (Points) Conversion as function of time for relaxation data from runs RG10, RG11, RG12, and RG13 of Ballard *et al.*,[15,42] in each case the fifth removal from γ-radiation source (data are therefore denoted RG10R5, *etc.*). Initial values of w_p were 0.87 (RG10R5), 0.87 (RG11R5), 0.83 (RG12R5), and 0.88 (RG13R5), initial $\bar{n} \approx 39$, 32, 62, and 61, final w_p 0.90, 0.90, 0.90, and 0.91, and final $\bar{n} \approx 13$, 12, 17, and 21, respectively. (Lines) Simulations using eq 30 with eq 22 for D^{rd} and the following fractions of desorbed free radicals undergoing aqueous-phase termination: 15% (RG10R5), 16% (RG11R5), 4% (RG12R5), and 18% (RG13R5).

the relationship[15]

$$\frac{[M_{aq}]}{[M_{aq}]^{sat}} = \left(\frac{[M]}{[M]^{sat}}\right)^{y} \tag{29}$$

in which the superscript "sat" refers to the fully saturated ("interval II") value. Only through use of eq 29 can the correct values of [M] (and, if necessary, $[M_{aq}]$) be calculated for use in the radical balance and conversion differential equations. For MMA and a number of other monomers,[27] $y \approx 0.6$. The empirical functional form of eq 29 fits a range of experimental data and is in accord with rigorous thermodynamic treatment.[56] For MMA, $[M]^{sat}$ = 6.6 mol dm^{-3} and $[M_{aq}]^{sat}$ = 0.15 mol dm^{-3}.[15]

Results of Simulating MMA Emulsion Polymerizations

γ-Radiolysis Relaxations: High Conversion. The first data to be simulated come from MMA γ relaxations at values of w_p such that the system either is, or nearly is, glassy (*i.e.*, for $w_p \gtrsim 0.82$). Figures 3 and 4 show the results of fitting four separate relaxation experiments, these being the last relaxations in the runs denoted RG10, RG11, RG12, and RG13 by Ballard *et al.*[15,42] In all of these simulations, $\rho_{thermal}$ was taken as zero (simulations with the $\rho_{thermal}$ value used for intermediate conversion, discussed later, show negligible difference), while on account of the considerations given above, p = 1 was used. To begin with (the results of Figure 3), the assignment $X_c^0 = 50$ was made.[34] For reasons that will soon become apparent, the data fitting at high conversion is insensitive to the values (within reasonable bounds) of k_p^1, X_c^0, and pD_{mon}.

Figure 3 compares experimental and simulated conversion as a function of time for a relaxation commencing at a high w_p: 0.88. It can be seen that the completely *a priori* model discussed above, which contains *no adjustable parameters*, reproduces the data extremely well. Moreover, exact agreement can be obtained by minor adjustments to the parameters. One example of this is shown in Figure 3: by merely increasing D^{rd} by a factor of 3 above that predicted by the completely *a priori* model of eq 22, the experimental data are reproduced quite acceptably. The said parameter adjustment is equivalent to increasing the radius of interaction for residual termination from the Lennard-Jones radius σ to 3σ. Such an increase is quite reasonable if, on the slow encounter time scales of reaction diffusion, chain ends are not completely immobile.[34] If eq 22 for D^{rd} is retained, equally excellent accord (Figure 4) can be obtained in simulating experiment by allowing some aqueous-phase termination to occur, specifically, by giving $\rho_{re\text{-}entry}$ a value 0.82 that of eq 16, which would entail 18% of desorbed free radicals terminating in the aqueous-phase. Given the extremely high $\bar{n}$ of these high-conversion relaxations (see captions to Figures 3 and 4), this too is a plausible result, as already discussed. If a higher than expected rate of termination by reaction diffusion is the actual explanation here, then such an "elevated" termination rate should also be observed in equivalent bulk and suspension (for example) polymerizations. Careful analysis of such polymerization data should therefore help in distinguishing between the mechanistic proposals of this paragraph.

Figure 4 compares experimental and simulated high-conversion relaxation data for a range (admittedly not extensive) of different initial values of w_p. The simulations were made to agree with experiment in these instances by allowing for a small percentage of aqueous-phase termination of desorbed free radicals. (In each case equally good reproduction could be obtained by allowing the reaction diffusion reaction radius to be increased, as in Figure 3.) It can be seen that for three of these data sets essentially the same fraction of aqueous-phase termination yields excellent accord with experiment. The exception is the run with the lowest initial w_p, RG12R5, where the fitted fraction of aqueous-phase termination is significantly smaller. This single discrepancy could be ascribed to the higher (on average) aqueous-phase concentration of monomer during this relaxation (see eq 29). This would imply that desorbed free radicals are more likely to propagate, and thence re-enter a particle, rather than terminate. Alternatively, the discrepancy might be artifactual: this relaxation was begun during the final stages of the Trommsdorff acceleration regime, during which MMA experimental kinetics are notoriously difficult to measure accurately.

Next we state what can be learned from our high-conversion simulations. It is basically that, as has already been indicated on several occasions, chain-length-dependent termination plays absolutely no role in high-conversion MMA kinetics. We know this because we per-

formed simulations in which D_{mon} was increased by a factor of 10 (thereby increasing all values of D_i^{com} by this amount) and in which k_{tr} was increased by about a factor of 2 (so increasing the fraction of short free radicals). In both cases absolutely no differences in the simulated kinetics were discernible. This observation can only mean that high-conversion MMA termination kinetics are completely dominated by the rate coefficient for long–long termination, which is of course the reaction diffusion termination rate coefficient. The reason for this is simply that at high conversions D_{mon} ($=D_1^{com}$) is less than an order of magnitude greater than D^{rd} (whereas, before the glass transition, $D_{mon} \gg D^{rd}$). Given how D_i^{com} decreases with i (see eq 23), one thus has that $D_i \approx D^{rd}$ for all but the very shortest chains. Hence, essentially all termination interactions occur at the reaction diffusion (long–long) rate. This result might otherwise be expressed through saying that long–long termination dominates overwhelmingly the high-conversion rate of termination. An upshot of this is that parameters such as k_p^1 are kinetically irrelevant at high conversions.

Because of the above finding, it is logical to suggest that these high-conversion systems might be very accurately described by the simple, chain-length-independent, "pseudo-bulk" equation that is conventionally used to describe (chain-length-independent) termination:

$$\frac{d\bar{n}}{dt} = \rho - \beta k_{tr}[M]\bar{n} - 2c^{LL}\bar{n}^2$$

$$\frac{d[R^\bullet]}{dt} = 2fk_d[I] - 2k_t^{LL}[R^\bullet]^2 \quad (30)$$

Simulating the relaxation kinetics using eq 30 (with reentry taken into account using eq 17) gives results that are in accord to much better than 1% in radical concentration with those of the full chain-length-dependent simulation using the same parameters. Hence, under these conditions eq 30 provides an absolutely acceptable representation of the complete results, and in fact was used to generate all of the results of Figure 4. It is stressed that under the present circumstances there is nothing nonmicroscopic about using eq 30, for the k_t of this equation is a microscopic one and one which has been shown to be accurate for almost all discrete termination reactions. However, it is emphasized that this simplification of being able to ignore the chain-length dependence of termination kinetics is only possible in glassy systems.

The most important conclusion from this section is that *termination at high conversion is completely dominated by chain encounter through reaction diffusion (i.e., through long–long termination)*. Although this result permits great simplifications in the kinetics to be made, it could only be reached through first carrying out complete, chain-length-dependent modeling.

Chemical Initiation: High Conversion. We next turn to modeling high-conversion, chemically initiated data. For the reasons given above, this modeling can be performed with the simple pseudo-bulk equation, eq 30. Although the experiments modeled were actually begun in interval II ($w_p = 0.33$), we restrict our attention here to their high conversion parts ($w_p \geq 0.85$). Thus, we commence our modeling well after the brief transient following addition of initiator, which has been shown to contain significant contributions from inhibition effects[15] and which no attempt is made to model.

The parameter values used in fitting these intermediate-conversion data were, where appropriate, those found above to be successful in modeling high-conversion γ relaxations. Now, the latter data could be fitted either by varying pD_{mon} or the amount of aqueous-phase termination. Probably the more likely is that in which the radius of interaction for residual termination is increased. Also, if a small fraction of exited free radicals does terminate in the aqueous phase at high conversion, then this fraction would be expected to vary according to such factors as the rate of exit, the initiator concentration in the aqueous phase, and so on. This means that the fractions found above for relaxation conditions would not necessarily be applicable under conditions of chemical initiation. The value of k_t^{LL} influences only the intraparticle kinetics, however, and thus a value of it used in modeling relaxations should be directly applicable for modeling of chemically initiated experiments. Thus we here use exactly the parameters of the fit of Figure 3: $\rho_{thermal} = 0$, $\rho_{re\text{-}entry}$ given by eq 16, and D^{rd} assigned a value 3 times the prediction of eq 22. This leaves $\rho_{initiator}$ as the only unknown; the fitted values of this quantity will be used to furnish a test of a model for entry[27] discussed previously.

Table I. Values of Entry Rate Coefficients Found from Fitting High-Conversion, Chemically Initiated Data[a]

run	range of $\bar{n}$	range of w_p	$[S_2O_8^{2-}]$, 10^{-3} mol dm^{-3}	fitted $\rho_{initiator}$, s^{-1}	efficiency, %
RC10	5.9–21.2	0.85–0.93	4.6	0.087	66
RC73	15.0–44.8	0.85–0.91	8.8	0.35	75
RC82	14.0–44.3	0.85–0.92	4.7	0.24	96
RC83	9.9–15.0	0.85–0.89	2.4	0.096	76

[a] Ranges of $\bar{n}$ and w_p are experimental values at beginning and end of regime used for modeling.

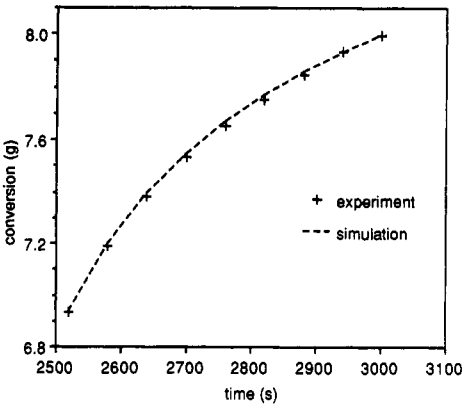

Figure 5. (Points) Conversion as function of time for initiation by persulfate for run RC10.[15,42] (Line) Simulation with eq 30. Parameters are as in Table I and text.

Results of this fitting are given in Table I, and a comparison of fitted and experimental results for a particular run appears in Figure 5. Note that the four experiments of Table I represent a variety of experimental conditions. So, for instance, the particle number in run RC10 was about twice that of run RC82—hence the different ρ values in this case. Also given in Table I are the efficiencies of initiation implied by the fitted values of $\rho_{initiator}$. These efficiencies have been calculated from the entry rate coefficient for 100% initiator efficiency (which is $\rho_{initiator} = 2k_d[I]N_A/N_c$; see eq 15). In these calculations $k_d = 1.3 \times 10^{-6}$ s^{-1} at the reaction temperature of 50 °C was taken.[57]

It must be borne in mind in the evaluation of the results of Table I that the actual values of the efficiency given there are somewhat uncertain (perhaps ±30%). This is because of uncertainties (i) in some of the model parameters used to deduce the experimental value of $\rho_{initiator}$ and (ii) because the value of k_d in an emulsion polymerization system may be slightly different from that measured in pure systems. Nevertheless, it is clear from Table I that

the fitted values of the entry rate coefficient are all only slightly less than is predicted by assuming 100% initiator efficiency and the quoted k_d, *i.e.*, that the efficiency is very high. This high efficiency for MMA can be contrasted to that for styrene, which is of the order of 1% (depending on [I]). In the case of styrene, extensive data for $\rho_{initiator}$ were quantitatively fitted by the model of eq 15, with a value of z between 2 and 3.[27] Exactly the same model predicts[27] for MMA that initiator efficiency should be closer to 100%, as indeed found here. In fact, using recommended values for MMA[27] (specifically, $z = 4$), and taking [M] = 1.7 mol dm^{-3} (as appropriate for $w_p = 0.85$) and [I] as for RC83, eq 15 predicts an efficiency of 61% in the present instance. Given the above-mentioned parameter uncertainties, the accord here between fitted and predicted values for ρ provides convincing evidence for the correctness of the entry model leading to eq 15. It also provides confirmation of the correctness for the method and parameters used in the present modeling, since the values of $\rho_{initiator}$ in Table I were obtained entirely by fitting, without any reference to any model for initiator efficiency.

γ-Radiolysis Relaxation: Intermediate Conversion. We now turn to modeling γ-relaxation data in the intermediate-conversion regime, *i.e.*, when the w_p value is well below that where the glass transition occurs ($w_p < 0.82$). For this task we use the full chain-length-dependent equations, eqs 2–4. This is because it is now expected that the effects of chain-length-dependent termination will be kinetically important, for from Figure 2 it is evident that now D_{mon} will be many orders of magnitude greater than D^{rd} and thus that D_i^{com} values will be important in determining the overall rate of termination. The modeling strategy adopted was to seek parameters to fit a typical γ-relaxation run (which are especially sensitive to chain-stopping events) and then see if the same parameters (augmented where necessary) also fit relaxations starting at different values of w_p. The relaxation run chosen for this "baseline" fitting was the fourth removal from the source of run RG13 of Ballard *et al.*[15,42] This relaxation had an initial w_p value of 0.51 and initial $\bar{n} = 7.5$. The parameters deemed to be variable were $\rho_{thermal}$, k_p^1, X_c, and pD_{mon}. All other parameters were fixed as above (in particular, D^{rd} was given by eq 22 and $\rho_{re\text{-}entry}$ by eq 16).

The first choice made for X_c^0 was a value of 50, the value of the entanglement spacing j_c^0 in MMA.[34,41] The first estimate of k_p^1 was taken as the long-chain value (see above), that of p as 1, that of D_{mon} as measured by PFG NMR (*i.e.*, as in Figure 2), and $\rho_{thermal} = 10^{-2}$ s^{-1}. Results are shown in Figure 6 (line a). It can be seen immediately that these parameters give far too rapid a relaxation compared to that observed experimentally. This means that either the simulated rate of termination is too high or the simulated rate of radical production is too low. As a first attempt to reproduce experiment, X_c was reduced to 1 (thereby reducing the simulated rate of termination)—line b in Figure 6, in which the relaxation is still too rapid. The next measure was therefore to increase $\rho_{thermal}$—line c in Figure 6. Now the relaxation is not too rapid, but the simulated kinetics are qualitatively different from experiment (Figure 6 only shows a small selection of the extensive number of simulations that were carried out). It was possible to reproduce exactly the experimental kinetics with a number of parameter sets (*e.g.*, lines d and e of Figure 6). However, one perhaps surprising result is that parameter values could not be set arbitrarily and other parameters varied so as to reproduce experiment. This finding should be evident from the above descriptions

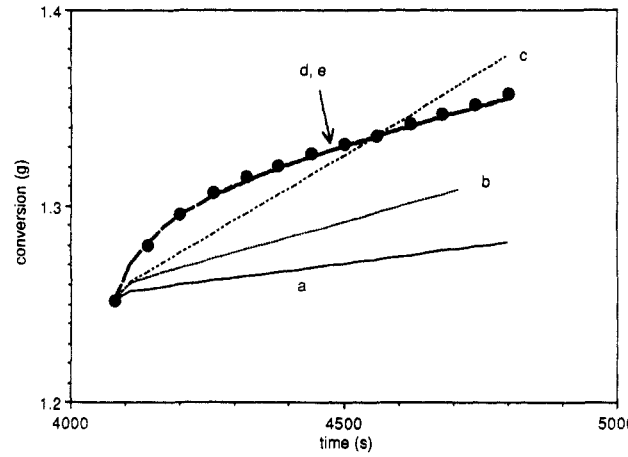

Figure 6. Conversion as function of time for fourth removal from γ source of run RG13.[15,42] Initial $w_p = 0.51$, initial $\bar{n} \approx 7.5$. (Points) Experiment. (Lines) (simulation values for d and e are indistinguishable on this scale):

	$\rho_{thermal}$, s^{-1}	X_c	pD_{mon}/D_{mon}(NMR)	k_p^1/k_p
(a)	10^{-2}	50 (X_c^0)	1	1
(b)	10^{-2}	1	1	1
(c)	5×10^{-2}	1	1	1
(d)	10^{-3}	1	0.12	1
(e)	10^{-3}	1	0.25	10

of modeling, in which it was made clear that simply varying $\rho_{thermal}$ could not lead to data reproduction. Certainly this nonarbitrariness is a quality which enhances the utility of our model. In the end it was found that *only* with $\rho_{thermal} = 1 \times 10^{-3}$ s^{-1} and $X_c = 1$ could the data be reproduced (obviously small variations in these values could be tolerated). As shown in Figure 6, with these values and with $k^{p1} = k_p$, pD_{mon} needed to be reduced to $0.12D_{mon}$(NMR) to fit the data (where D_{mon}(NMR) is that shown in Figure 2), while with $k_p^1 = 10k_p$, $pDm_{on} = {}^1/_4D_{mon}$(NMR) was required.

Now we turn to the physical resonableness of these fitted (but not absolutely unique) parameter values. The initial parameter set (line a of Figure 6) showed too rapid a relaxation, clearly because short free radicals were "too effective" at terminating. The rate of such termination can be reduced by any of the following: reducing the diffusion coefficient of a monomeric free radical, increasing the rate at which a monomeric free radical grows into a slower-moving dimer (or trimer, *etc.*), and decreasing the diffusion coefficients of higher oligomers compared with that of monomer. Thus, the values of D_{mon}, k_p^1 (and k_p^2, *etc.*), and X_c are linked in the effect their variation has on a simulation. X_c obviously cannot be made any lower than 1, and the value of D_{mon} that was used is probably accurate. However, it is possible that k_p^i values could be larger than those used here for small i. Although simulations showed that further increasing k_p^1 above the value $10k_p$ had almost no effect on the kinetics (with this k_p^1, monomeric radicals become dimeric almost instantaneously), if k_p^2 (and k_p^3, *etc.*) was made somewhat larger, then values of X_c and p higher than 1 and 0.25, respectively, could be used to model the data. Being no more than an exercise in curve fitting, this was not attempted here. Another consideration to be borne in mind is that our method of specifying D_i^{com} for a grain must overestimate, if anything, the true rate of termination (see text under eq 23). In any case, we stress in particular that the parameter values used for line e of Figure 6, *viz.* $X_c = 1$, $p = 0.25$, and $k_p^1/k_p = 10$, are physically reasonable. Needless to say it is important that accord can be obtained with such a reasonable parameter set and all other model values as given *a priori*. Also, the desirability of having

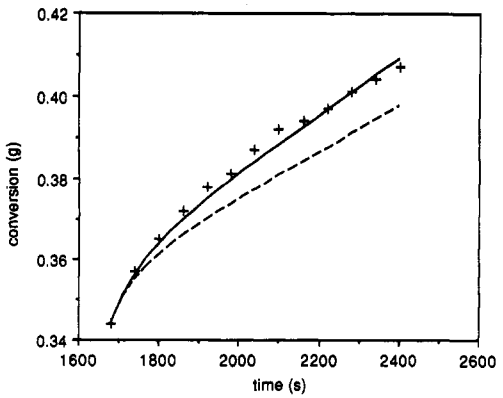

Figure 7. Fitting γ-relaxation data at intermediate conversion: second (w_p = 0.33) relaxation of run RG13.[15,42] (Points) Experiment. (Lines) Using parameters of simulation e of Figure 6 (broken line); (full line) as for simulation e of Figure 6 except $pD_{mon} = 0.18D_{mon}$(NMR).

better known values of parameters such as D_i^{com} and k_p^i will hopefully spur experiments in these directions. The values of p and σ (both possibly a function of the chain lengths i and j) are also clearly of importance in the modeling of termination rates, and so it would of course be ideal if polymerization modeling could be attacked with independently known experimental values of these quantities. Experimental work aimed at determining the values of all these important microscopic parameters is therefore important for both the use and the development of the theory of this paper.

It is apparent that termination interactions at intermediate conversions overwhelmingly involve one short, mobile free radical and one longer, far less mobile radical. This has been exhibited through the extreme sensitivity of simulations to the values of k_p^1 and pD_{mon}. Considerable variation in the rate of termination by reaction diffusion (as in the previous section) gave essentially identical kinetics. This gives rise to the following physical picture: intermediate-conversion termination occurs when the rapid diffusion of a short radical results in it encountering a long free radical, long free radicals constituting the vast majority of the overall radical population. Furthermore, because our simulations were of relaxations, in which rates of new radical generation are low, the short free radicals involved in short–long termination must have mostly arisen as a result of transfer (more complex and exact analyses of results confirm this conclusion[50]). This will also be true in standard chemically initiated polymerizations at intermediate conversion, although in these the proportion of short–long interactions involving a short species directly arisen from initiation will be a little larger. These insights into termination have been reached as a result of the complete (chain-length-dependent) simulation approach we have here adopted.

Next we examine whether the physically reasonable parameters of the above modeling can be used predictively. To do this, the "optimal" parameters for the fit to relaxation data at w_p = 0.51 (*i.e.*, those for line *e* in Figure 6) were used to calculate relaxation behavior at the lower w_p of 0.33. The simulation results were then compared with the corresponding experimental data (the second relaxation of experiment RG13). It should be noted that the relaxation at this lower w_p exhibits more rapid termination than that at higher w_p; *i.e.*, these relaxations show different experimental kinetic behaviors. The results of our new modeling are shown in Figure 7. It can be seen that the comparison between fitted and experimental results is quite good, with excellent accord being achieved by reducing the value of pD_{mon} by about 30%. Given the uncertainties in the various components for the calculation, this is regarded as providing some confirmation of the correctness of the overall model and its component parameters.

We conclude this section by emphasizing the difficulties in modeling intermediate conversion polymerizations over an extensive range of w_p. In modeling a γ relaxation, one is fortunate in that the range of w_p that is traversed is small; thus, uncertain parameter values that are expected to vary with w_p can reasonably be held constant, so rendering modeling a meaningful exercise (as was the case above). However, in modeling experiments that span a range of w_p, conversion dependences of parameters must be known accurately. Particularly telling in this respect is the lack of good data for D_{mon} in the range $0.65 < w_p < 0.85$ (see Figure 2) and of D_i/D_{mon}, to which the modeling is sensitive.

Effect of Introducing Segmental Termination. By assigning the reaction diameter of a monomer unit as the radius of interaction in calculating the rate coefficient for translational diffusion-controlled termination, the chain-end encounter step in termination is effectively subsumed into the translational diffusion step of this process. While our model is able to reproduce data at intermediate and high conversion, it does not appear to be adequate in the limit of zero conversion. This is because if one uses parameters that are reasonable for zero conversion in our model (which obviously entails altering the exponents in eq 23) and calculates the average termination rate coefficient as given by eq 14, a value is obtained that is about an order of magnitude greater than the typical value of 10^7 dm^3 mol^{-1} s^{-1} observed experimentally for MMA (and styrene) at zero conversion.

This is perhaps disturbing, because $\langle k_t(w_p=0)\rangle$ is usually identified as representing the rate coefficient for segmental termination in this low-w_p regime (in which chain-end encounter is thought to be rate-determining). Since segmental motions would intuitively be expected to become slower as polymer concentration increases with increasing w_p, the segmental diffusion rate would be expected to decrease. Hence, our model prediction in intermediate-w_p simulations that (for example) $k_t^{11} > \langle k_t(w_p=0)\rangle$ possibly casts doubt in our data fitting. One possible resolution of this conundrum is to speculate that $\langle k_t(w_p=0)\rangle$ values may not in fact represent rate coefficients for segmental termination. Rather, the rate of termination at low w_p may simply be controlled by the rate of center-of-mass translational diffusion of free radicals.

Given these observations, it was decided to investigate the consequences of incorporating a finite rate coefficient for the chain-end encounter step in performing simulations of polymerizations. This was done in the following crude fashion. First, the segmental component to the termination rate coefficient k_t^{ij}(seg) was assumed to be chain-length-independent, and, second, this k_t(seg) was assigned the (w_p-independent) value $\langle k_t(w_p=0)\rangle$. These assumptions are no doubt flawed, but there seem no more reasonable options available at present, for it is concentrations well above c^{**} that here interest us (the many available models of segmental termination all hold for dilute solution conditions only). The center-of-mass translational diffusion contribution to the termination rate coefficient, which we temporarily denote k_t^{ij}(diff), was calculated using eq 18 exactly as before, and the overall

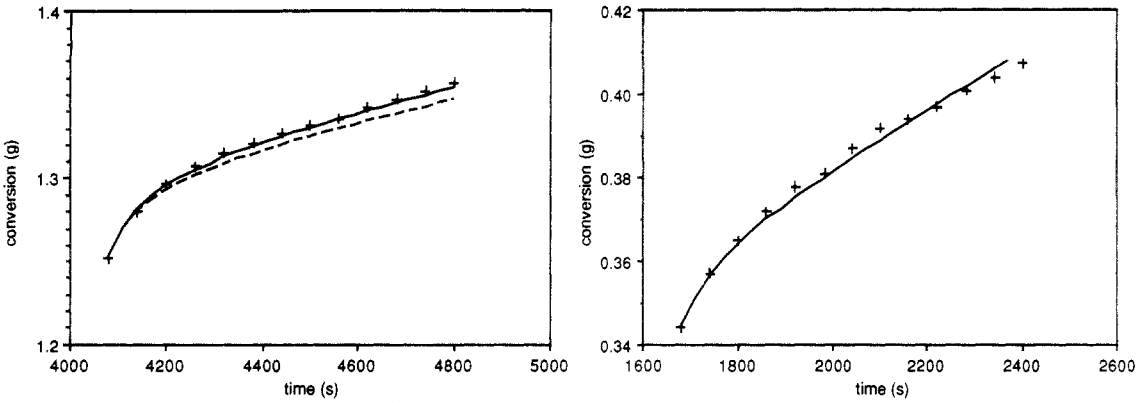

Figure 8. Fitting intermediate-conversion, γ-relaxation data from run RG13[15,42] (parametrization incorporating $\langle k_t(w_p=0)\rangle$—see eq 31—used). (Points) Experiment. (Lines) Simulation with parameter set as in text. (Right-hand diagram) Second ($w_p = 0.33$) relaxation, $pD_{mon} = D_{mon}$(NMR). (Left-hand diagram) Fourth (initial $w_p = 0.51$) relaxation; (broken line) $pD_{mon} = D_{mon}$(NMR); (full lines) $pD_{mon} = 0.8D_{mon}$(NMR).

value of k_t^{ij} then evaluated using

$$\frac{1}{k_t^{ij}} = \frac{1}{k_t^{ij}(\text{diff})} + \frac{1}{\langle k_t(w_p=0)\rangle} \tag{31}$$

In modeling the data with this alternative approach, parameter values were used as before, and $\langle k_t(w_p=0)\rangle$ was given the value 1.8×10^7 dm^3 mol^{-1} s^{-1}.[58] Results from fitting of the fourth and second relaxations of experiment RG13 are shown in Figure 8; in these simulations, $\rho_{thermal} = 10^{-3}$ s^{-1}, $X_c = 1$, $k_p^1 = k_p$, $p = 1$, and $\rho_{re\text{-}entry}$ as given by eq 16 were at first used. It can be seen that good accord was found for the $w_p = 0.33$ relaxation using this quite reasonable parameter set; for the $w_p = 0.51$ relaxation an optimal fit was obtained using $p = 0.8$, again a reasonable value.

On the basis of the findings of this section, it may perhaps be ventured that chain-end encounter needs to be specifically accounted for in modeling low- and intermediate-w_p polymerizations but can be ignored at higher w_p (where only reaction diffusion is significant). However, such a conclusion is very problematic, for at intermediate conversions the polymer segment density is uniform, and so the concept of a chain-end encounter step being *slower* than the chain encounter step is hard to justify. Besides, our modeling clearly shows that short–long interactions dominate the intermediate conversion termination rate, and it is hard to imagine any segmental diffusion process coming strongly into play for such interactions, except in possibly increasing slightly the radius of interaction that we have here used (see the discussion on radius of interaction). For these reasons the physical implications of the modeling done in this section are unclear. What is perhaps suggested is that whatever it is that makes $\langle k_t(w_p=0)\rangle$ values as *low* as they are found to be also serves to lower intermediate-conversion termination rates. Interestingly, in the calculations alluded to above in which the ideas of this paper were used to try to calculate $\langle k_t(w_p=0)\rangle$, $p = 1$ was assumed. However, for $p = 0.25$, the calculated $\langle k_t(w_p=0)\rangle$ values are very close to experimental values.

Conclusion

In this paper we have first presented a model for the kinetics of free-radical polymerization which takes specific account of the dependence of the termination rate coefficient on radical chain length. Our objective was to develop a *complete* and *accurate* microscopic description of polymerization kinetics, one which could nevertheless be implemented for the study of experimental polymerization systems. The complexity of this task is a consequence of microscopic completeness and accuracy. We have, however, more than demonstrated that our model is tractable. Additionally, through our maximal use of current chemical physics knowledge, the model contains a minimum (at this stage) of adjustable parameters. Further, putting our model to use requires only very modest computational resources.

In concluding this paper, we first emphasize the *methodology* of this work. As far as kinetic equations are concerned, this is set out in a number of ways in eqs 2–4 and 7–11, while the most important aspects of how to specify parameter values for use in these kinetic equations are to be found in eqs 5, 6, and 15–25.

The fitting here is felt to have provided a stern test of the model for chain-length-dependent termination and its component parameters. This is because data (from γ relaxations) sensitive to termination events were deliberately chosen for modeling, and most of the parameters used in the fitting are either known to reasonable accuracy or can be estimated with relatively small uncertainty. Indeed, that all parameter values by physically reasonable was insisted upon at all times. Moreover, our fitting procedure was to use parameters obtained in one system (*e.g.*, a relaxation at a particular conversion) to predict behavior under significantly different conditions (*e.g.*, a relaxation at a quite different conversion). It is especially noteworthy that a completely *a priori* molecular level model for termination in the glassy regime,[34] one containing no adjustable parameters, predicts the high-conversion relaxation behavior with relative success (recalling that the value of the termination rate coefficient can vary over 7 orders of magnitude). Further, this model becomes very accurate when comparatively minor, and physically reasonable, parameter adjustments are made to it. The parameter values were certainly not found to be unique in fitting data; however, neither were arbitrary parameter variations possible for fitting purposes. Because all model parameters are microscopic, the potential exists for all fitted parameters to be tested and evaluated through independent experiments. In this vein, we note that our data fitting gave results totally in accord with the predictions of a well-tested theory for initiator efficiency in emulsion polymerizations.[27]

The above successes notwithstanding, it must be admitted that the rectitude of all aspects of our polymerization model has not been proven here beyond doubt. It is possible that our model contains imperfections and that, in modeling experimental data, these imperfections have been masked by the parameter variation that has been

allowed. It should nevertheless be clear that every effort has been made to keep our model as correct as possible, and so we feed our modeling results can be regarded with some confidence, even if not absolute certainty.

In this paper we have used our model to cast light on the mechanism of termination over a wide range of conversions. These results can be summarized as follows:

(1) At high conversion (*i.e.*, at and beyond the glass transition), termination overwhelmingly involves two long entangled chains encountering at the reaction diffusion rate.

(2) At intermediate conversions (say, from $w_p \approx 0.1$ to near the glass transition, which covers most conversions in emulsion and bulk polymerizations), termination predominantly involves a long, entangled chain and a much more mobile short, relatively unentangled chain, these latter often arising from *transfer*.

(3) At low conversions (say, w_p well less than 0.1, *i.e.*, the initial stages of a bulk polymerization), the majority of termination events involve a chain of moderate to long degree of polymerization and a shortish chain, more often than not directly arisen from *initiator*.

It is emphasized that none of the above descriptions are absolute (*e.g.*, not *all* termination events at intermediate conversions are short–long). However, when used properly, the above insights can be used to better understand polymerization phenomena. To take an important example, the origin of the Trommsdorff–Norrish or gel effect can be cast in terms of short–long termination. Specifically, the decrease in *average* k_t which gives rise to and sustains this rate acceleration must result from *short* chain diffusion coefficients decreasing. This decrease has two aspects: (1) as w_p increases, segmental friction coefficients decrease, thereby slowing down short-chain diffusion; and (2) as w_p increases, short chains become entangled at lower and lower degrees of polymerization, thereby giving a lower population of short free radicals to effect short–long termination. One sees that to attempt to encapsulate the Trommsdorff effect in a single parameter, as many have tried to do, is almost certainly a nonphysical oversimplification of a phenomenon that is to be properly understood in terms of a whole spectrum of D_i^{com} values. Full modeling studies of the type done here would appear to be the best way of properly handling the kinetics of low and intermediate conversions.

There is good reason to believe that the model of this paper can be used predictively, although completely *a priori* modeling is not advisable without some parameter adjustment based on fits to one or two "benchmark" data sets. Also, the model as given is only reliable above c^{**} and, therefore, as it stands here should be used circumspectly at very low conversions. It is apparent that the modeling that has been done reinforces the conclusion of many[1,3–11,59] that accurate, reliable quantification and prediction of free-radical polymerization kinetics must take into account the dependence of the termination rate on chain length. A simple treatment which ignores this effect can *only* be used meaningfully for modeling glassy systems.

Our results and methods can clearly be used for wider purposes, such as suggesting qualitative and quantitative strategies for polymer preparation and properties, for example, controlling residual monomer and molecular weight distribution (including the presence of oligomeric chains).

Acknowledgment. G.T.R. acknowledges the receipt of an Australian Postgraduate Research Award. The financial support of the Australian Research Grants Committee is gratefully acknowledged. Paul Callaghan is thanked for the PFG NMR measurements of D_{mon} for MMA.

References and Notes

(1) Benson, S. W.; North, A. M. *J. Am. Chem. Soc.* **1962**, *84*, 935.
(2) Schulz, G. V. *Z. Phys. Chem. (Munich)* **1956**, *8*, 290.
(3) Cardenas, J.; O'Driscoll, K. F. *J. Polym. Sci., Polym. Chem. Ed.* **1976**, *14*, 883.
(4) Cardenas, J.; O'Driscoll, K. F. *J. Polym. Sci., Polym. Chem. Ed.* **1977**, *15*, 1883.
(5) Tulig, T. J.; Tirrell, M. *Macromolecules* **1981**, *14*, 1501.
(6) Soh, S. K.; Sundberg, D. C. *J. Polym. Sci. Polym. Chem. Ed.* **1982**, *20*, 1299.
(7) Olaj, O. F.; Zifferer, G.; Gleixner, G. *Macromolecules* **1987**, *20*, 839.
(8) Bamford, C. H. *Eur. Polym. J.* **1989**, *25*, 683.
(9) Mahabadi, H. K. *Macromolecules* **1985**, *18*, 1319.
(10) Mahabadi, H. K. *Macromolecules* **1991**, *24*, 606.
(11) Russell, G. T.; Gilbert, R. G.; Napper, D. H. *Macromolecules* **1992**, *25*, 2459.
(12) Ley, G. J. M.; Schneider, C.; Hummel, D. O. *J. Polym. Sci., C: Polym. Lett.* **1969**, *27*, 119.
(13) Lansdowne, S. W.; Gilbert, R. G.; Napper, D. H.; Sangster, D. F. *J. Chem. Soc., Faraday Trans. 1* **1980**, *76*, 1344.
(14) Ballard, M. J.; Gilbert, R. G.; Napper, D. H. *J. Polym. Sci., Polym. Lett. Ed.* **1981**, *19*, 533.
(15) Ballard, M. J.; Napper, D. H.; Gilbert, R. G. *J. Polym. Sci., Polym. Chem. Ed.* **1984**, *22*, 3225.
(16) Asua, J. M.; Sudol, E. D.; El-Aasser, M. S. *J. Polym. Sci., A: Polym. Chem.* **1989**, *27*, 3903.
(17) Casey, B. S.; Morrison, B. R.; Maxwell, I. A.; Gilbert, R. G.; Napper, D. H. Free-radical exit in emulsion polymerization: I. Theoretical model. *J. Polym. Sci., Polym. Chem. Ed.* **1993**, submitted for publication.
(18) Nomura, M.; Harada, M. *J. Appl. Polym. Sci.* **1981**, *26*, 17.
(19) Ugelstad, J.; Hansen, F. K. *Rubber Chem. Technol.* **1976**, *49*, 536.
(20) Casey, B. S.; Morrison, B. R.; Gilbert, R. G. The role of aqueous-phase kinetics in emulsion polymerizations. *Prog. Polym. Sci.* **1993**, in press.
(21) Morrison, B. R.; Casey, B. S.; Lacík, I.; Leslie, G. L.; Sangster, D. F.; Gilbert, R. G.; Napper, D. H. Free-radical exit in emulsion polymerization. II. Model discrimination via experiment. *J. Polym. Sci., Polym. Chem. Ed.* **1993**, submitted for publication.
(22) Gilbert, R. G.; Napper, D. H. *J. Macromol. Sci., Rev. Macromol. Chem. Phys. C* **1983**, *23*, 127.
(23) Hawkett, B. S.; Napper, D. H.; Gilbert, R. G. *J. Chem. Soc., Faraday Trans. 1* **1980**, *76*, 1323.
(24) Mills, M. F.; Gilbert, R. G.; Napper, D. H.; Croxton, C. A. Spatial inhomogeneities in emulsion polymerizations: Repulsive wall calculations. *Macromolecules* **1993**, in press.
(25) Mills, M. F.; Gilbert, R. G.; Napper, D. H.; Rennie, A. R.; Ottewill, R. H. SANS studies of morphology. *Macromolecules* **1993**, in press.
(26) Mills, M. F.; Gilbert, R. G.; Napper, D. H. *Macromolecules* **1990**, *23*, 4247.
(27) Maxwell, I. A.; Morrison, B. R.; Napper, D. H.; Gilbert, R. G. *Macromolecules* **1991**, *24*, 1629.
(28) Asua, J. M.; de la Cal, J. C. *J. Appl. Polym. Sci.* **1991**, *42*, 1869.
(29) Nomura, M.; Harada, M.; Eguchi, W.; Nagata, S. *J. Appl. Polym. Sci.* **1971**, *15*, 675.
(30) Whang, B. C. Y.; Napper, D. H.; Ballard, M. J.; Gilbert, R. G.; Lichti, G. *J. Chem. Soc., Faraday Trans. 1* **1982**, *78*, 1117.
(31) Ugelstad, J.; Mørk, P. C.; Dahl, P.; Rangenes, P. *J. Polym. Sci., C: Polym. Lett.* **1969**, *27*, 49.
(32) Penboss, I. A.; Gilbert, R. G.; Napper, D. H. *J. Chem. Soc., Faraday Trans. 1* **1986**, *82*, 2247.
(33) Gilbert, R. G.; Smith, S. C. *Theory of Unimolecular and Recombination Reactions*; Blackwell Scientific: Oxford, U.K., 1990.
(34) Russell, G. T.; Napper, D. H.; Gilbert, R. G. *Macromolecules* **1988**, *21*, 2133.
(35) Piton, M. C.; Gilbert, R. G.; Chapman, B. E.; Kuchel, P. W. *Macromolecules* **1993**, in press.
(36) Tirrell, M. *Rubber Chem. Technol.* **1984**, *57*, 523.
(37) de Gennes, P.-G. *Scaling Concepts in Polymer Physics*; Cornell University: Ithaca NY, 1979.
(38) de Gennes, P.-G. *Macromolecules* **1981**, *14*, 1637.
(39) de Gennes, P.-G. *J. Chem. Phys.* **1971**, *55*, 572.
(40) Wheeler, L. M.; Lodge, T. P.; Hanley, B.; Tirrell, M. *Macromolecules* **1987**, *20*, 1120.

(41) Bueche, F. *Physical Properties of Polymers*; Interscience: New York, 1962.
(42) Ballard, M. J. Ph.D. thesis, University of Sydney, 1988.
(43) Casey, B. S.; Mills, M. F.; Sangster, D. F.; Gilbert, R. G.; Napper, D. H. *Macromolecules* **1992**, *25*, 7063.
(44) Russell, G. T.; Napper, D. H.; Gilbert, R. G. *Macromolecules* **1988**, *21*, 2141.
(45) Buback, M.; Garcia-Rubio, L. H.; Gilbert, R. G.; Napper, D. H.; Guillot, J.; Hamielec, A. E.; Hill, D.; O'Driscoll, K. F.; Olaj, O. F.; Shen, J.; Solomon, D.; Moad, G.; Stickler, M.; Tirrell, M.; Winnik, M. A. *J. Polym. Sci., Polym. Lett. Ed.* **1988**, *26*, 293.
(46) Mahabadi, H. K.; O'Driscoll, K. F. *J. Macromol. Sci. A, Chem.* **1977**, *11*, 967.
(47) Whang, B. C. Y.; Ballard, M. J.; Napper, D. H.; Gilbert, R. G. *Aust. J. Chem.* **1991**, *44*, 1133.
(48) Morrison, B. R.; Maxwell, I. A.; Gilbert, R. G.; Napper, D. H. In *ACS Symposium Series Polymer Latexes—Preparation, Characterization and Applications*; Daniels, E. S., Sudol, E. D., El-Aasser, M., Eds.; ACS Symposium Series 492; American Chemical Society: Washington, DC, 1992; p 28.
(49) Callaghan, P. Private communication.
(50) Russell, G. T. Ph.D. thesis, University of Sydney, 1990.
(51) Leest, Y.; Smets, G. *J. Polym. Sci., Polym. Chem. Ed.* **1988**, *26*, 913.
(52) Berens, A. R.; Hopfenberg, H. B. *J. Membr. Sci.* **1982**, *10*, 283.
(53) Kosfeld, R.; Schlegel, J. *Angew. Makromol. Chem.* **1973**, *29/30*, 105.
(54) Faldi, A.; Tirrell, M.; Lodge, T. P.; von Meerwall, E. D. *Polym. Prepr.* **1991**, *32*, 400.
(55) Blackley, D. C. *Emulsion Polymerisation*; Applied Science: London, 1975.
(56) Maxwell, I. A.; Kurja, J.; van Doremaele, G. H. J.; German, A. L.; Morrison, B. R. *Makromol. Chem.* **1992**, *193*, 2049.
(57) Kolthoff, I. M.; Miller, I. K. *J. Am. Chem. Soc.* **1951**, *73*, 3055.
(58) Tulig, T. J.; Tirrell, M. *Macromolecules* **1982**, *15*, 459.
(59) Adams, M. E.; Russell, G. T.; Casey, B. S.; Gilbert, R. G.; Napper, D. H.; Sangster, D. F. *Macromolecules* **1990**, *23*, 4624.
(60) Ballard, M. J.; Gilbert, R. G.; Napper, D. H.; Pomery, P. J.; O'Donnell, J. H. *Macromolecules* **1984**, *17*, 504.